small
NANO MICRO

Spatially Selecting a Single Cell for Lysis Using Light-Induced Electric Fields

Christian Witte, Clemens Kremer, Mayuree Chanasakulniyom, Julien Reboud, Rab Wilson, Jonathan M. Cooper, and Steven L. Neale**

The selective lysis of single cells is one of the major bottlenecks in the analysis of rare cells or targeted populations in complex biological samples such as blood or biopsies, and more especially so in miniaturized systems[1–5]. Whilst there have been advances in sequencing,[6] expression profiling[7] and metabolite analysis[8] at the single cell level, new techniques for single cell lysis are still challenging. Microfluidic lysis strategies are primarily based on mechanical,[9] chemical[10–12] and electric[13,14] methods, with a particular focus on bulk sample treatment rather than targeted single cell lysis. Electrical methods that aim at single cell lysis require exceptionally good control of the position of the cell of interest relative to the microelectrodes to trigger lysis.[15–17] Optical techniques, usually based on intense laser excitation (kW), are thought to arise as a consequence of the creation of a plasma by energy absorption in the liquid, followed by the emission of a shockwave and a cavitation event, resulting in a mechanical event close to the cell of interest (although cavitation bubbles create wider lysing areas.[18,19] Other, alternative methods, involving either chemical gradients[10,11,20,21] or acoustic forces,[22–24] result in responses that are widely distributed in space, leading to limited specificities in a dense or confluent population of cells.

Recently, a new concept based on optically induced electric fields, also called 'optoelectronic tweezers' (OET)[25] has been applied to achieve electroporation and lysis for single cells.[26,27] Instead of conventional metal electrodes, a photosensitive material is utilized as a "virtual" electrode. A data projector or laser can be applied to selectively illuminate the photoconductor, creating localized electric field gradients. Lin et al.[26] demonstrated lysis of oral cancer and fibroblast cells. However, a significant lysis rate was only achieved with high optical powers of 10^5 W cm^{-2} and large illumination patterns (above 50 μm, for cells with a diameter <20 μm), restricting the application of the system to diluted samples with cells considerable distances apart (10s of microns). Furthermore, this system required the use of low conductivity solutions and exposing samples to non-physiological conditions, causing stress to the cells and perturbing intracellular processes.

In this work we describe the integration of an amorphous silicon (aSi) photoconductor electrode into a microfluidic environment and demonstrate the creation of highly localized electric-field gradients suitable for the selection of single cells for lysis from within a dense cell population. Furthermore, for the first time, this single cell lysis method based on light induced electric fields is applied to both suspension and adherent cells under physiological conditions.

Compared to previous studies,[26,27] by reducing the beam spot by an order of magnitude to 2.5 micrometers and integrating a microchannel (allowing a reduction in the scale of the fluidic environment), we are now not only able to spatially select cells from within dense or confluent populations, but have demonstrated lysis with greatly reduced power densities, five orders lower (1 W cm^{-2} compared with 10^5 W cm^{-2}).[26] Although exposing cells to high light intensities, in the range of MWcm^{-2}, can be damaging,[28] the comparatively low intensities that we use ensures we are well below the threshold where the light by itself will affect the cells. The geometric aspects of the integrated chip, including the reduced volume (and subsequent reduced solution resistances), coupled with local changes in impedances induced by the contact between the cell and the photoconductor, have all enabled us to perform these experiments under physiological conditions.

Further, the advantage of our technique over conventional single cell lysis using metal microelectrodes, is that by inducing the electric field optically, we have a highly flexible approach where the single cell can be selected in a dynamic fashion (see **Figure 1** and Movie M1 in the Supporting Information). Transportation, positioning or localisation of the target cell, relative to the microelectrode is not necessary, as we bring the "electrode" to the chosen cell. Using a simple PowerPoint interface with a mouse and data projector, we position the optical spot on a displayed image of the cells, moving the electrode to the chosen position (see Figure 1 a and b). The technique therefore also negates the need for additional, complex fabrication and alignment steps in positioning the microelectrode array within a channel, when using conventional single cell electroporation.

In our configuration, we showed that when the beam spot is reduced to a few micrometers, the electric field strength is highly non-uniform with high magnitudes well defined

C. Witte, C. Kremer, M. Chanasakulniyom, J. Reboud, R. Wilson, J. M. Cooper, S. L. Neale
University of Glasgow
Division of Biomedical Engineering
G12 8LT, Scotland
E-mail: c.witte.1@research.gla.ac.uk;
steven.neale@glasgow.ac.uk

DOI: 10.1002/smll.201400247

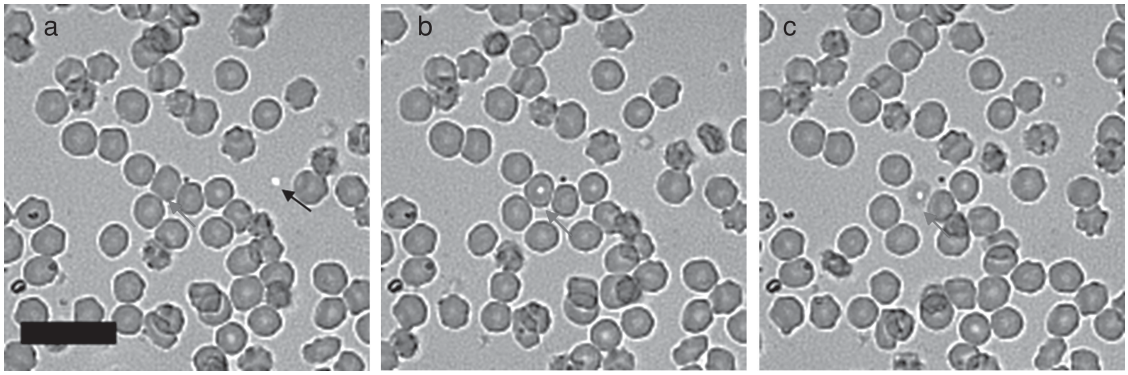

Figure 1. Single cell lysis of RBC at 25 KHz 20 V in PBS buffer (see movie M1 in ESI). (a) 2.5 µm beam spot (marked by black arrow) is used for selective lysis of target cell (red arrow). (b) Beam spot is focused on centre of cell. (c) Lysis complete after 25s. Scale bar: 25 µm.

close to the surface of the photoconductor. We evaluated the nature of this electric field in our device by performing a 2D simulation using COMSOL (v3.5, COMSOL Ltd., UK). **Figure 2** shows the simulated electric field contours created by a 2.5 µm light spot. Magnitudes of up to 16 kV cm^{-1} for an applied voltage of 20 V and frequency of 25 KHz in a low conductivity medium (10 mS m^{-1}) can be achieved. The Full Width Half Maximum (FWHM) was 4.6 µm (Figure 2b), showing that we can precisely control the electrical fields with the optical pattern. The transmembrane potential of red blood cells (RBCs) placed in this configuration shows a significant asymmetry with respect to the distance to the photoconductor, where the membrane closest to the 'virtual' electrode experiences a much higher drop (Figure S1 in ESI) that leads to lysis. Figure S2 in the Supporting Information shows that lysis time lies below 1 min, even for the smaller sizes (<9 µm), while Figure S3 (and Movie M2) show sequential targeted lysis in a dense population. These figures are discussed in more details in the Supporting Information.

After optimising the operation of the optoelectronic chip using a low conductivity buffer (Figures S1-S3), we replaced the buffer solution with a physiological, higher conductivity medium (>1 S m^{-1}). In this configuration, the applied voltage was found to drop mostly across the photoconductor while the field in the sample solution was significantly weaker. In **Figure 3**a, a comparison of the field produced by 2.5 µm beam spot in low and high conductivity buffer shows that the field strength in a high conductivity buffer is two magnitudes lower. This suggests that the potential across the cell membrane induced by the weak field in the solution would not be sufficient for lysis.[29]

However, as the cell membrane is a good insulator, the close distance between cell and photoconductor will change the impedance at the interface photoconductor/liquid significantly (the impedance change on electrodes due to adhesion of cells, proliferation or migration and their detection has previously been successfully demonstrated by electric cell-substrate impedance sensing).[30,31]

We modelled the transmembrane potential of the cell's dependence on the vertical distance between it and the photoconductor and considered the biconcave shape of a red blood cell (RBC). The closest distance to the electrode we considered was 5 nm and the furthest was 640 nm referring to the edge of the RBC (see Figure 3c –physiological distances range below 140 nm[33]. The results of our model show that the transmembrane potential is below the average threshold voltage for cell lysis of 1 V[32] for distances of >100 nm (Figure 3b).

A significant change in transmembrane voltage was observed in the simulations when reducing the cell-substrate distance to tens of nanometers. An increase in the potential of an order of one magnitude is obtained for gaps <10 nm. Previous studies have shown that, for buffer solutions with high conductivities, the electrostatic repulsion between the cells and the electrode is reduced, which promotes molecular contact to surfaces.[33] Consistent with this, we observe significant increases in the transmembrane voltage when the cell is in close contact with the surface. Furthermore, our model

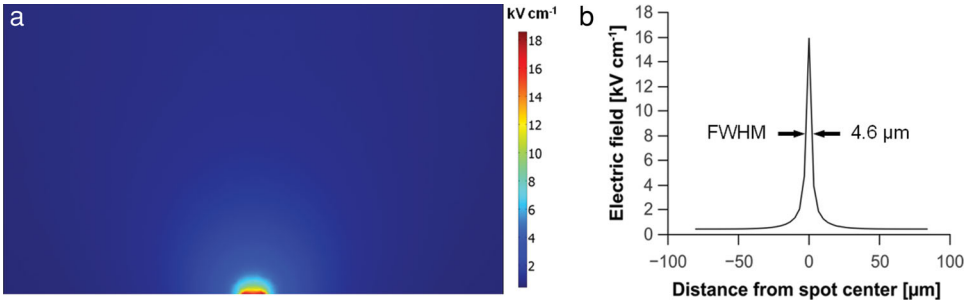

Figure 2. (a) Simulated non-uniform electric field (kV cm^{-1}) created by 2.5 µm spot in the microchannel (35 µm distance between the ITO electrode and photoconductor) when a voltage of 20 V and 25 kHz is applied. (b) Corresponding FWHM of the area of higher electric field created by the 2.5 µm light spot.

DOI: 10.1002/smll.201400247

NANO MICRO small

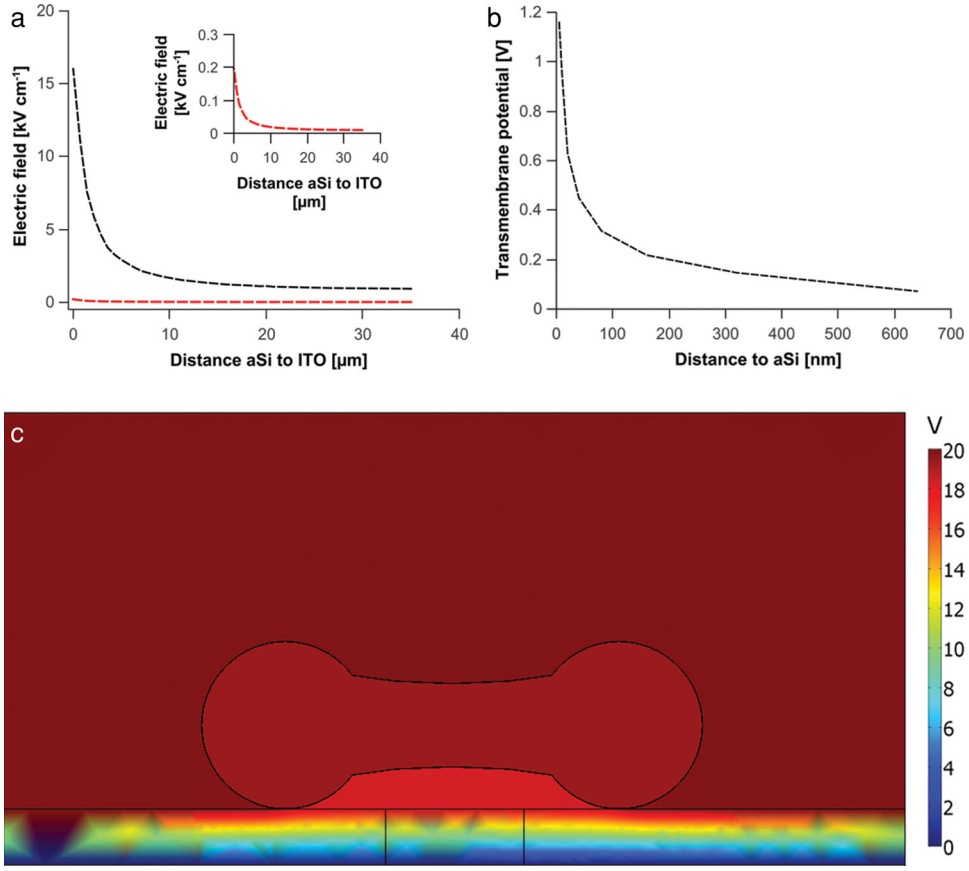

Figure 3. (a) Comparison of simulated electric field strength created by a 2.5 µm beam spot in low (10 mS m^{-1}, black curve) and high (PBS, 1.4 S m^{-1}, red curve) conductivity buffer is dependent on the distance between the amorphous silicon (aSi) layer and the ITO electrode. Inset shows detailed view of red curve. (b) Modelled transmembrane voltage of a RBC in PBS. The distance between the cell and the photoconductor surface was varied between 5 nm and 640 nm. (c) Plot of the electrical potential around a RBC that is 5 nm above the photoconductor at the closest (edge of RBC) and 700 nm at the furthest point (centre of RBC). A frequency of 25 KHz and an applied voltage signal of 20 V were used.

shows a significant potential change in the liquid underneath the cell, which arises as a consequence of the high impedance of the cell membrane, which is dominating at close distances, and which results in an increased voltage drop and field strength at the interface.

Figure 1 (and Movie M1) confirms the simulations, showing the successful targeted lysis of RBCs suspended in high conductivity media (PBS), using a 2.5 µm diameter beam and an applied voltage of 20 V (25 KHz). The time for lysis was <1 min. The process is linked to the irreversible formation of pores, causing the release of intracellular components. RBCs are well suited for observing the loss of cellular integrity, as the high intracellular concentration of haemoglobin produces a strong contrast relative to the surroundings, when the cell is intact. Figure 1 shows that the targeted cell lost its contrast and faded away over time, leaving behind only the empty membrane or "ghost" of the cell.

Furthermore, while suspension cells, including circulating cancer cells or white blood cells are interesting targets for single cell studies,[34] the majority of the mammalian cells grow on surfaces. If adherent cells need to be transferred into an analytical device by suspending them first, the activation of signalling pathways related to the environmental change can lead to perturbation of biological processes and might influence the experimental outcome.[35] Therefore, a planar substrate onto which cells adhere prior to lysis can improve the biological quality and relevance of the analysis. The amorphous silicon we use as a photoconductor has a thin natural oxide layer on its surface, so that the cells are grown on a glass-like surface, a commonly used cell culture substrate.

We show the first demonstration of lysis of adherent cell lines with light-patterned electrical fields. Breast cancer cell line (MCF7) was injected into the chip and incubated overnight (37 °C, 5% CO_2), resulting in small clusters of cells on the photoconductor surface immersed in cell culture medium (0.95 mS m^{-1}). We used a 5.5 µm diameter optical spot to verify if lysis could be achieved. In **Figure 4**(a-c), a large cluster of cells is lysed within 80 s, by moving the light spot over each cell, while selective lysis can be easily achieved by only pacing the light spot on a single cell, as shown in Figure 4(d-f), where a MCF7 cell in the centre of a cluster is lysed within 35 s.

This study shows that light patterned electrical fields can be used for single cell lysis, in dense populations of cells, and uniquely, under physiological conditions. A well-defined high electric field area was created by using a small optical spot (2.5 micrometers in diameter) and integrating the photoconductor into a microfluidic chamber, thus reducing and precisely controlling the distance between the top and bottom electrodes. Selective lysis of target cells

DOI: 10.1002/smll.201400247

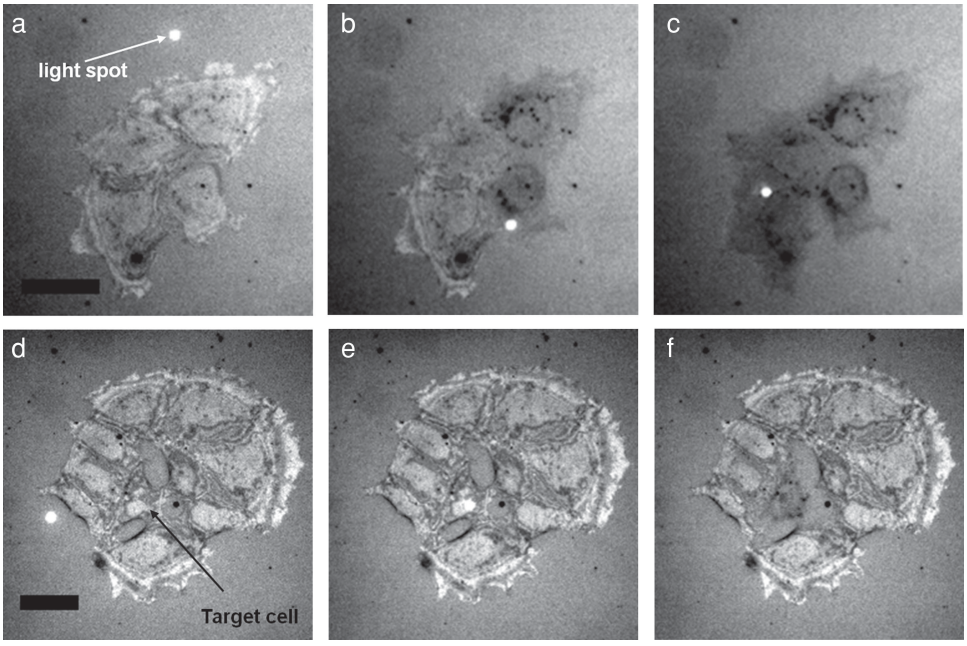

Figure 4. MCF7 cells adhered to the surface of the photoconductor and immersed in culture medium inside the optoelectronic chip. (a-c) A 5.5 µm beam spot is used to achieve lysis within 80 s in a cluster of cells at 25 KHz, 20 V. (d-f) A cell in the centre of a cluster is targeted and lysed using an applied voltage signal of 20 V at 25 KHz. Lysis is achieved after 35 s. Scale bars: 30 µm, see movies M3 and M4 in ESI.

in physiological solutions was achieved within 1 minute of exposure and this was demonstrated on non-adherent cells, RBCs, and on adherent cells, MCF7s. We propose that the ability to lyse cells in high conductivity solution is linked to the decreased distance between the cell's membrane and the photoconductor, which causes a greater potential drop across the membrane. As the surface of our device is a flat glass-like layer, it provides a promising system for the growth of adherent cell lines and their precisely controlled, selective lysis, releasing their intracellular contents for further biomolecular analysis.

Experimental Section

Optoelectronic Chip Fabrication: Indium tin oxide (ITO) coated (600 nm) microscope slides (25 × 75 × 1 mm) and cover slips (22 × 40 × 0.17 mm) (diamond coatings, UK) were used for the fabrication of the optoelectronic chip. The microscope slides were coated with a 1 µm amorphous silicon (a-Si) layer by plasma-enhanced chemical vapour deposition using pure silane gas (10 W, 300 mTorr, 250 °C, 15 sccm). The substrates were then used to create a sandwich structure with a negative photoresist. SU8 3050 (MicroChem Corp., USA) was spin coated (4000 rpm) onto the a-Si modified microscope slide and placed on a hotplate at 95 °C.

The ITO coated cover slip containing predrilled holes (to enable microfluidics interconnects) was bonded immediately to the uncured SU8 film by carefully placing it on top. This was followed by a soft bake at 95 °C for 25 minutes. The SU8 photoresist was exposed (MA6 mask aligner, SÜSS MicroTec AG, DE) through a polymer-emulsion film mask aligned to the predrilled holes in the cover slip for 60 seconds. A post-exposure bake at 65 °C for 2 minutes and 95 °C for 5 minutes was performed prior to developing the unexposed SU8 through the drilled inlet and outlet holes using Microposit EC solvent (Shipley, USA).

The fabrication process in itself is novel, providing a method to integrate an optelectronic substrate within microfluidic channels and achieving bonding and packaging, in a single step. Previous techniques used a subsequent bonding step after photopatterning of the resist.[26,27,36] An epoxy glue was applied to the resist to enable the assembling of the electrode substrates. The need for a precise application of the glue and the bonding of the substrates without unwanted filling or blockage of the channel by the epoxy glue make this technique cumbersome. Importantly, our technique provides control over the dimensions of the fluidic channels and

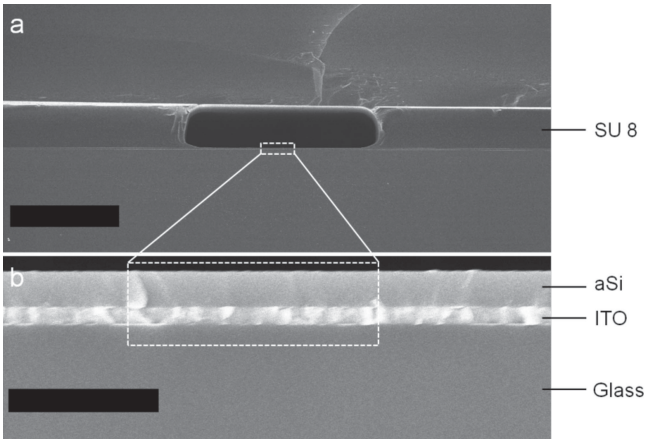

Figure 5. Cross sections of optoelectronic chip showing (a) SU8 photoresist sandwiched between the electrode substrates and (b) expanded view of the bottom electrode substrate with amorphous silicon (a-Si) and indium tin oxide (ITO) layer. Scale bar 100 µm and 5 µm, respectively.

DOI: 10.1002/smll.201400247

NANO MICRO small

Table 1. Parameter used in the model.

Parameter	Value	Parameter	Value
Channel cross section W x H [μm]	200 × 35	Conductivity a-Si (light state) [S m^{-1}]	$1.4 \cdot 10^{-3}$
Frequency [KHz]	25	Permittivity of a-Si	14
Amplitude [V]	20	Cell membrane thickness [nm]	7
Conductivity media [S m^{-1}]	0.01, 1.4	Conductivity cell membrane [S m^{-1}]	$1 \cdot 10^{-6}$
Permittivity media	79	Permittivity cell membrane[37]	12.5
Thickness amorphous silicon [μm]	1	Conductivity cytosol [S m^{-1}]	0.8
Conductivity a-Si (dark state) [S m^{-1}]	$1.8 \cdot 10^{-5}$	Permittivity cytosol	60

voids, which have a significant impact on the electric field strength (see Figure S1 and accompanying discussion in ESI, where we show how transmembrane voltage is dependent upon geometric dimensions under constant electrical parameters). In this work, the resulting height of the microfluidic void was 35 μm, giving an experimental cell chamber volume of 740 pL. **Figure 5**(a-b) shows the cross section of the sandwich structure and the electrode layers in the optoelectronic chip.

Electric connections were made via exposed ITO areas using silver paint (Agar Scientific, UK). The microchip was connected to a function generator (TG5011, TTi, UK). An Olympus microscope (BX52, Olympus, Japan) equipped with a dual port (U-DP) and an Orca Flash4.0 CMOS-camera (Hamamatsu, Japan) were used for recording. A DELL data projector (Dell 1510X) connected to a PC with presentation software (Microsoft PowerPoint) was used to generate virtual electrode projections through a 40× objective (PlanN, NA: 0.65, FN: 22, Olympus, Japan) onto the photoconductor. The positions of the lysis spots were simply controlled by mouse movement or arrow keys on the keyboard. Figures 1 and 4 show results of experiments using upright brightfield reflective microscopy with varying brightness levels.

Preparation of Cells: Human blood samples were provided by the local Blood Transfusion Service (Glasgow) and were stored at 4 °C prior to use. For low conductivity media experiments, blood cells were washed once in PBS, followed by three washing steps in a buffer solution made of 8.5% w:v sucrose, 0.3% w:v glucose and 3 mM Hepes (pH 7.4, 10 mS m^{-1}) at 1500 rpm for 5 min. For the experiments in PBS buffer, blood cells were washed once in PBS. Blood samples were manually introduced in the microchip using a pipette.

MCF7 cells were cultured in DMEM containing 10% fetal calf serum (v:v), 4.5 g l^{-1} glucose, 2 mM L-glutamine, 1% penicillin and streptomycin (v:v). After manual injection of the MCF7 cells, the optoelectronic chip was placed in a petri dish and incubated overnight at 37 °C (5% CO_2). The morphological change of a cell upon exposure to the electric field was monitored and timed (see movies in supporting information).

Simulations of Electric Fields and Membrane Potentials: Simulations for electric field strength and transmembrane potentials in RBCs were performed using COMSOL (v3.5, COMSOL Ltd., UK). A 2D cross sectional model of the chip and a single-shelled RBC were used to simulate the electric fields and resulting transmembrane potentials. The thin outer shell represents the cell's membrane (7 nm lipid bi-layer) and the core represents the intracellular contents (cytosol). **Table 1** shows the parameters used. The conductivity of the amorphous silicon was expressed as a saturated Gaussian (whose maximum corresponds to the illuminated areas on the photoconductor, produced by light from the data projector).[37]

Supporting Information

Supporting Information is available from the Wiley Online Library or from the author.

Acknowledgements

Dr. Neale acknowledges the support of an Engineering and Physical Sciences Research Council (EPSRC)/Royal Academy of Engineering research fellowship, grant number EP/G058393/1. This work was also supported by the EPSRC grants EP/K027611/1 and EP/I017887/1. The authors thank Dr. Lisa C. Ranford-Cartwright and Elizabeth Peat (Institute of Biomedical and Life Sciences, Division of Infection and Immunity, Glasgow Biomedical Research Centre, University of Glasgow) for the access to blood samples. We thank the James Watt Nanofabrication Center (Glasgow, UK) for help with device fabrication.

[1] S. Lindström, H. Andersson-Svahn, *Lab Chip* **2010**, *10*, 3363.
[2] D. Ryan, K. Ren, H. Wu, *Biomicrofluidics* **2011**, *5*, 021501.
[3] C. E. Sims, N. L. Allbritton, *Lab Chip* **2007**, *7*, 423.
[4] M. A. Walling, J. R. Shepard, *Chem. Soc. Rev.* **2011**, *40*, 4094.
[5] D. Wlodkowic, J. M. Cooper, *Anal Bioanal. Chem.* **2010**, *398*, 193.
[6] C. Zong, S. Lu, A. R. Chapman, X. S. Xie, *Science* **2012**, *338*, 1622.
[7] L. Flatz, R. Roychoudhuri, M. Honda, A. Filali-Mouhim, J. P. Goulet, N. Kettaf, M. Lin, M. Roederer, E. K. Haddad, R. P. Sekaly, G. J. Nabel, *Proc. Natl. Acad. Sci. U. S. A.* **2011**, *108*, 5724.
[8] A. Amantonico, P. L. Urban, R. Zenobi, *Anal. Bioanal. Chem.* **2010**, *398*, 2493.
[9] Z. Lin, Z. Cai, *Biotechnol. J.* **2009**, *4*, 210.
[10] D. Di Carlo, C. Ionescu-Zanetti, Y. Zhang, P. Hung, L. P. Lee, *Lab Chip* **2005**, *5*, 171.
[11] E. A. Schilling, A. E. Kamholz, P. Yager, *Anal. Chem.* **2002**, *74*, 1798.
[12] P. Sethu, M. Anahtar, L. L. Moldawer, R. G. Tompkins, M. Toner, *Anal. Chem.* **2004**, *76*, 6247.
[13] C. Church, J. Zhu, G. Huang, T. R. Tzeng, X. Xuan, *Biomicrofluidics* **2010**, *4*, 44101.

DOI: 10.1002/smll.201400247

[14] G. Mernier, N. Piacentini, T. Braschler, N. Demierre, P. Renaud, *Lab Chip* **2010**, *10*, 2077.
[15] F. Han, Y. Wang, C. E. Sims, M. Bachman, R. Chang, G. P. Li, N. L. Allbritton, *Anal. Chem.* **2003**, *75*, 3688.
[16] S. Kemmerling, S. A. Arnold, B. A. Bircher, N. Sauter, C. Escobedo, G. Dernick, A. Hierlemann, H. Stahlberg, T. Braun, *J. Struct. Biol.* **2013**, *183*, 467.
[17] Y. Nashimoto, Y. Takahashi, T. Yamakawa, Y. S. Torisawa, T. Yasukawa, T. Ito-Sasaki, M. Yokoo, H. Abe, H. Shiku, H. Kambara, T. Matsue, *Anal. Chem.* **2007**, *79*, 6823.
[18] R. B. Brown, J. Audet, *J. R. Soc. Interface* **2008**, *5*, S131,
[19] K. R. Rau, P. A. Quinto-Su, A. N. Hellman, V. Venugopalan, *Biophys. J.* **2006**, *91*, 317.
[20] P. C. H. Li, D. J. Harrison, *Anal. Chem.* **1997**, *69*, 1564.
[21] J. T. Nevill, R. Cooper, M. Dueck, D. N. Breslauer, L. P. Lee, *Lab Chip* **2007**, *7*, 1689.
[22] T. Tandiono, D. S. Ow, L. Driessen, C. S. Chin, E. Klaseboer, A. B. Choo, S. W. Ohl, C. D. Ohl, *Lab Chip* **2012**, *12*, 780.
[23] T. C. Marentis, B. Kusler, G. G. Yaralioglu, S. J. Liu, E. O. Haeggstrom, B. T. Khuri-Yakub, *Ultrasound Med. Biol.* **2005**, *31*, 1265.
[24] M. T. Taylor, P. Belgrader, B. J. Furman, F. Pourahmadi, G. T. A. Kovacs, M. A. Northrup, *Anal. Chem.* **2001**, *73*, 492.
[25] P. Y. Chiou, A. T. Ohta, M. C. Wu, *Nature* **2005**, *436*, 370.
[26] Y.-H. Lin, G.-B. Lee, *Appl. Phys. Lett.* **2009**, *94*, 033901.
[27] J. K. Valley, S. Neale, H. Y. Hsu, A. T. Ohta, A. Jamshidi, M. C. Wu, *Lab Chip* **2009**, *9*, 1714.
[28] K. C. Neuman, E. H. Chadd, G. F. Liou, K. Bergman, S. M. Block, *Biophys. J.* **1999**, *77*, 2856.
[29] C. Kremer, C. Witte, S. L. Neale, J. Reboud, M. P. Barrett, J. M. Cooper, *Angew. Chem. Int. Ed.* **2014**, *53*, 842.
[30] I. Giaever, C. R. Keese, *Proc. Natl. Acad. Sci. U. S. A.* **1984**, *81*, 3761.
[31] J. Hong, K. Kandasamy, M. Marimuthu, C. S. Choi, S. Kim, *The Analyst* **2011**, *136*, 273.
[32] J. C. Weaver, *J. Cell. Biochem.* **1993**, *51*, 426.
[33] A. Trommler, D. Gingell, H. Wolf, *Biophys. J.* **1985**, *48*, 835.
[34] S. L. Faley, M. Copland, D. Wlodkowic, W. Kolch, K. T. Seale, J. P. Wikswo, J. M. Cooper, *Lab Chip* **2009**, *9*, 2659.
[35] J. Seidl, R. Knuechel, L. A. Kunz-Schughart, *Cytometry* **1999**, *36*, 102.
[36] Y.-H. Lin, G.-B. Lee, *Sens. Actuators, B* **2010**, *145*, 854.
[37] S. L. Neale, A. T. Ohta, H. Y. Hsu, J. K. Valley, A. Jamshidi, M. C. Wu, *Opt. Express* **2009**, *17*, 5232.

Received: January 28, 2014
Revised: February 27, 2014
Published online:

DOI: 10.1002/smll.201400247